

R. & M. No. 3222

LIBRARY
ROYAL AIRCRAFT ESTABLISHMENT
BEDFORDS

R. & M. No. 3222



MINISTRY OF AVIATION

AERONAUTICAL RESEARCH COUNCIL
REPORTS AND MEMORANDA

Some Notes on the Zero-Lift Wave Drag of Slender Wings with Unswept Trailing Edge

By J. WEBER

LONDON: HER MAJESTY'S STATIONERY OFFICE

1961

PRICE: 14s. od. NET

Some Notes on the Zero-Lift Wave Drag of Slender Wings with Unswept Trailing Edge

By J. WEBER

COMMUNICATED BY THE DEPUTY CONTROLLER AIRCRAFT (RESEARCH AND DEVELOPMENT),
MINISTRY OF AVIATION

*Reports and Memoranda No. 3222**

December, 1959

Summary. Minimum values of the zero-lift wave drag of slender wings with certain fixed properties have been calculated by slender-body theory. The cross-sectional area distributions of the wings are taken to be polynomials and the fixed properties of the wings correspond to fixed first and second derivatives of the area distributions at the apex and rear end.

The drag for delta wings of rhombic cross sections has also been calculated by thin-wing theory without the slenderness assumption. Comparisons between the drag coefficients calculated by both theories have been made for a series of wings to investigate the applicability of slender theory.

The calculations by both theories suggest that it should be possible to design thickness distributions which have drags as low as that of the so-called Lord V area distribution on plan-forms for which the Lord V distribution is unsuitable. Further, this can be achieved when the thickness near the apex and the slope at the trailing edge are restricted.

1. *Introduction.* We consider in this Report the wave drag due to volume of wings with unswept trailing edges. We use the term wing in a general sense namely for configurations which are winglike towards the trailing edge.

The question arises: how low can the wave drag of a slender wing of given length, span and volume be for a given free-stream Mach number? In the design of aircraft, certain restrictions are imposed on the geometry of the wings, for instance by requiring a minimum thickness at certain stations. For this Report, we have chosen the first and second streamwise derivatives of the cross-sectional area distribution at the apex and at the trailing edge as the properties to be prescribed. Applying slender-body theory, we determine in Section 2 for certain families of area distributions the minimum drag for fixed values of some of these parameters.

Since slender-body theory predicts in certain cases even negative drag values, it seems necessary to investigate the validity of the theory. The slenderness assumption can be tested by comparing the drag values determined from supersonic thin-wing theory and from slender-thin-wing theory. (Slender-thin-wing theory gives the same drag value as slender-body theory.) We refrain from applying the full small perturbation theory (in which the boundary condition is satisfied on the surface instead of in the wing median plane) since the work involved would be too great. To apply even thin-wing theory to wings of general plan-form and cross section shapes is a rather lengthy process. We consider, therefore, in this Report wings of simple geometry, namely delta wings with rhombic cross sections. This is a large enough class of wings for the effect of various properties on

* Previously issued as R.A.E. Report No. Aero. 2630—A.R.C. 21,909.

the validity of the slenderness assumption to be studied. For wings where the centre section is given as a polynomial of 5th degree, with 4 independent parameters, we have calculated the zero-lift wave drag numerically for the slenderness parameter βs varying between 0.2 and 0.8. For a number of wings of this class, the drag values are compared with those from slender theory to determine the error in the drag estimate due to the slenderness assumption. Finally, we determine the minimum drag values from thin-wing theory, when some of the derivatives of the area distribution at the apex and trailing edge are fixed.

In this Report, no pressure distributions are calculated, which implies that we have not checked whether the flow assumed in the calculation can be realized in a viscous flow. We determine only the theoretical minimum of the wave drag under certain conditions to investigate what ranges of the parameters should be considered in designing for low drag in a real fluid.

2. *Wings with Minimum Wave Drag for Certain Fixed Properties of the Cross-Sectional Area Distribution According to Slender-Body Theory.* 2.1. *The General Drag Formula.* For wings with sharp straight trailing edges, the drag due to thickness is according to slender-body theory given by the relation (see for example Ref. 1):

$$\begin{aligned} \frac{D}{q} = & -\frac{1}{2\pi} \int_0^1 \int_0^1 S''(x)S''(x') \log |x - x'| dx dx' \\ & + \frac{S'(1)}{\pi} \int_0^1 S''(x) \log (1-x) dx \\ & + \frac{[S'(1)]^2}{2\pi} [k - \log \beta s] \end{aligned} \quad (1)$$

with

$$k = \log 2 - \frac{\int_{-1}^{+1} \int_{-1}^{+1} \epsilon(\eta)\epsilon(\eta') \log |\eta - \eta'| d\eta d\eta'}{\left[\int_{-1}^{+1} \epsilon(\eta) d\eta \right]^2} \quad (2)$$

where

$$\epsilon(y) = \left[\frac{\partial z(x, y)}{\partial x} \right]_{x=1} \quad (3)$$

and

$$\eta = y/s. \quad (4)$$

x, y, z is a rectangular co-ordinate system with x in the streamwise direction and z normal to the wing plane (*i.e.*, the plane through apex and trailing edge). The maximum chord c_0 is taken as unity. s is the semi-span of the wing at the trailing edge and $\epsilon(y)$ the spanwise distribution of the streamwise slope of the wing at the trailing edge. $S(x)$ is the area of the wing in cross sections $x = \text{constant}$, $S'(x)$ and $S''(x)$ are the first and second derivatives of $S(x)$ with respect to x .

We refer in the following the wave drag of a given configuration to the value of the minimum drag of a body of revolution of the same length c_0 and volume v , *i.e.*, to the drag of the corresponding Sears-Haack body

$$\left(\frac{D}{q} \right)_{S.H.} = v^2 \frac{128}{\pi} \quad (5)$$

and write:

$$\frac{D}{q} = K_0 v^2 \frac{128}{\pi} \quad (6)$$

2.2. *Special Drag Formulae.* In this Report, we consider wings with pointed plan-forms and sharp leading and trailing edges. The cross-sectional area distributions of such wings can be written in the form:

$$S(x) = x^2(1-x)f(x)$$

where $f(x)$ is a continuous function. To consider only polynomials for $f(x)$ is sufficiently general for the purpose of this Report.

If $S(x)$ is known as a polynomial in x , K_0 can be expressed in explicit form by using the values of

$$I_{nm} = - \int_0^1 \int_0^1 x^n x'^m \log |x - x'| dx dx' \quad (7)$$

which have been tabulated for $n, m \leq 9$ by G. G. Brebner in an unpublished Royal Aircraft Establishment paper. (Values of I_{nm} for $n, m \leq 4$ have been published in Ref. 2.) The values of I_{nm} are reproduced in Table 1.

Since the drag factor K_0 depends only on the area distribution and not on the volume, it is sufficient to consider area distributions of unit volume. We therefore consider the area distributions:

$$S(x) = x^2(1-x) \sum_{n=0}^N a_n x^n \quad (8)$$

where

$$\sum_{n=0}^N \frac{a_n}{(n+3)(n+4)} = 1. \quad (9)$$

For $N = 5$, the following relation exists between K_0 and the coefficients a_n^* :

$$\begin{aligned} K_0 = \frac{1}{256} \left\{ -\frac{5}{4} a_0^2 - \frac{23}{12} a_1^2 - \frac{55}{24} a_2^2 \right. \\ - \frac{307}{120} a_3^2 - \frac{83}{30} a_4^2 - \frac{617}{210} a_5^2 - \frac{7}{2} a_0 a_1 - \frac{13}{3} a_0 a_2 \\ - 5 a_0 a_3 - \frac{133}{24} a_0 a_4 - \frac{719}{120} a_0 a_5 - \frac{13}{3} a_1 a_2 \\ - \frac{29}{6} a_1 a_3 - \frac{127}{24} a_1 a_4 - \frac{3421}{600} a_1 a_5 - \frac{59}{12} a_2 a_3 \\ - \frac{79}{15} a_2 a_4 - \frac{841}{150} a_2 a_5 - \frac{161}{30} a_3 a_4 - \frac{169}{30} a_3 a_5 \\ \left. - \frac{86}{15} a_4 a_5 + \left[\sum_{n=0}^N a_n \right]^2 [k - \log \beta_s] \right\}. \quad (10) \end{aligned}$$

We introduce into Equation (10) the first and second derivatives of the area distribution at the apex and at the trailing edge. The first derivative at the apex is zero and at the trailing edge it is:

$$-S'(1) = \sum_{n=0}^N a_n. \quad (11)$$

* The constants are given as vulgar fractions instead of decimal numbers so that K_0 can be calculated correctly even in the cases where some $|a_n|$ are large numbers.

The second derivative has at the apex and at the trailing edge the values:

$$S''(0) = 2a_0, \quad (12)$$

$$-S''(1) = 2 \sum_{n=0}^N (n+2)a_n. \quad (13)$$

For $N = 3$ from Equations (9) to (13):

$$\begin{aligned} K_0 = \frac{1}{256} \left\{ 490 - \frac{7}{3} S''(0) - 63 [-S'(1)] + \frac{7}{3} [-S''(1)] \right. \\ + \frac{1}{60} [S''(0)]^2 + \frac{1}{60} [S''(1)]^2 - \frac{1}{60} S''(0)[-S'(1)] \\ + \frac{1}{120} S''(0)[-S''(1)] - \frac{17}{30} S'(1)S''(1) \\ \left. + [S'(1)]^2 \left[\frac{253}{120} + k - \log \beta s \right] \right\} \quad (14) \end{aligned}$$

and for $N = 5$:

$$\begin{aligned} K_0 = \frac{1}{256} \left\{ 907 \cdot 2 - 23 \cdot 1 S''(0) - 9 \cdot 96 a_1 - 1 \cdot 44 a_2 \right. \\ - 63 \cdot 6 [-S'(1)] + 1 \cdot 2 [-S''(1)] + \frac{25}{96} [S''(0)]^2 \\ + \frac{151}{600} a_1 S''(0) + 0 \cdot 04 a_2 S''(0) + 0 \cdot 325 S''(0)[-S'(1)] \\ + \frac{1}{120} S''(0)[-S''(1)] + \frac{11}{168} a_1^2 + \frac{23}{1050} a_1 a_2 \\ + \frac{53}{2100} a_1 [-S'(1)] + \frac{1}{105} a_1 [-S''(1)] + \frac{1}{525} a_2^2 \\ - \frac{1}{105} a_2 [-S'(1)] + \frac{1}{420} a_2 [-S''(1)] \\ - \frac{25}{84} [-S'(1)][-S''(1)] + \frac{1}{168} [S''(1)]^2 \\ \left. + [S'(1)]^2 \left[\frac{451}{840} + k - \log \beta s \right] \right\}. \quad (15) \end{aligned}$$

We refrain here from replacing the coefficients a_1 and a_2 by geometric terms such as the value and the position of the maximum cross-sectional area since this leads to even lengthier formulae for the drag.

2.3. Minimum Drag Values. For a given value of the free-stream Mach number, *i.e.*, given β , given ratio of semi-span to root chord, s , given k , we can determine the minimum drag factor by differentiating Equations (14) or (15) with respect to the terms that we do not intend to restrict.

For the numerical examples we choose wings with linear spanwise distributions of the streamwise slope at the trailing edge:

$$\epsilon(\eta) = \epsilon(0)(1 - |\eta|) \quad (16)$$

for which

$$k = \frac{25}{12} - \frac{1}{3} \log 2 \approx 1.85. \quad (17)$$

This special family of wings has been chosen since it provides for wings of delta plan-form the simple geometry desirable for the calculation of the drag factor by non-slender thin-wing theory.

Prescribing the behaviour of the area distribution at the trailing edge by prescribing $S'(1)$ and $S''(1)$, we obtain for $\beta s = 0.4$ the minimum drag factors plotted in Fig. 1. The envelope of the curves gives the lowest drag value for $\beta s = 0.4$, given $S''(1)$ and given degree of the polynomial expression for $S(x)$, Equation (8). The main feature of Fig. 1 is the fact that slender-body theory predicts a marked decrease of the smallest possible wave drag with increasing value of the second derivative of the area distribution at the trailing edge.

The curves of minimum drag for given $S''(1)$ are nearly the same for area distributions which are polynomials of 6th degree as for area distributions which are polynomials of 8th degree. We can therefore expect that an increase of the degree of the polynomial in the expression of the area distribution, Equation (8), to larger values would not reduce the minimum K_0 a great deal for the range of $S''(1)$ which is of practical interest, say $-S''(1) < 100$.

The minimum K_0 values for given $S'(1)$ and $S''(1)$ calculated for $N = 3$ and $N = 5$ differ more than the minimum K_0 for $N = 3$ and $N = 5$ when only $S''(1)$ is fixed. This suggests that for a higher degree of the polynomial for $S(x)$, Equation (8) (or any wider class of $S(x)$ than Equation (8) with $N = 3$ or 5), the choice of $S'(1)$ does not determine the minimum value of K_0 to the degree that a choice of $S''(1)$ does.

If one stays within the narrow class of area distributions given by Equation (8) with $N = 3$ or 5, and determines an area distribution which has given values of $S'(1)$ and $S''(1)$ say, one finds that in some cases the coefficients a_n are rather large and of varying sign, which usually entails rather bumpy $S(x)$ distributions. The pressure distributions on bodies with such area distributions would also be rather wavy. To investigate the pressure distributions for configurations which have for given $S''(1)$ a K_0 near the minimum, it would, therefore, not be advisable to do this for the area distributions which have been used for calculating the K_0 values plotted in Fig. 1. It would be desirable to choose (from a wider family) area distributions which vary slowly and have the required values of $S'(1)$, $S''(0)$, $S''(1)$. The K_0 values for such area distributions can be calculated by the numerical method of Ref. 3, which is an extension of Emlinton's method⁴ and includes area distributions with $S'(1) \neq 0$.

The minimum drag values for given values of the second derivative at the apex and at the trailing edge are plotted in Fig. 2. We notice that the minimum drag for given $S''(1)$ does not vary rapidly with a change of $S''(0)$.

The drag factors plotted in Figs. 1 and 2 are calculated for $\beta s = 0.4$. To illustrate the effect of the slenderness parameter, we have plotted in Fig. 3 the minimum K_0 for given $S''(1)$ and $N = 3$ for various values of βs .

The drag factors plotted in Figs. 1 to 3 are calculated for $k = 1.85$. Equation (1) shows that a decrease of k has the same effect as a decrease of $\log 1/\beta s$. For wings with sharp trailing edge, k depends only on the spanwise distribution of the streamwise slope at the trailing edge. A change from

a linearly varying $\epsilon(y)$ to a constant $\epsilon(y)$ reduces k from 1.85 to 1.5, which produces the same reduction of K_0 as an increase of βs from 0.4 to 0.57.

Let us finally compare the present results with the drag values of two particular area distributions which have been investigated in detail, experimentally and theoretically, on slender wings of various plan-forms. They are those of the so-called Newby-delta wing (wing I in Refs. 5 and 6) and the so-called Lord V area distribution (wing V in Refs. 5 and 6):

$$S(x) = 12x^2(1-x) \quad (18)$$

with

$$-S'(1) = 12, \quad S''(0) = 24, \quad -S''(1) = 48$$

and

$$S(x) = x^2(1-x)[28 - 42x + 28x^2 - 7x^3] \quad (19)$$

with

$$-S'(1) = 7, \quad S''(0) = 56, \quad -S''(1) = 14.$$

The drag factors of these area distributions for $k = 1.85$ and $\beta s = 0.4$ are:

$$\text{Wing I : } K_0 = 0.85$$

$$\text{Wing V : } K_0 = 0.74$$

A comparison of these K_0 values with the minimum values for the same $S''(1)$ plotted in Fig. 1 shows that the K_0 of wing I is considerably larger whilst the K_0 for wing V is close to the minimum value. If only $S''(1)$ were to be kept constant, the K_0 of wing I could be reduced either by decreasing $-S'(1)$ or by increasing $S''(0)$. The drag of wing V can be reduced noticeably only by allowing a larger value of $-S''(1)$. (As a consequence of the small difference between the minimum K_0 as a function of $S''(1)$ for area distributions given by polynomials of 6th degree and 8th degree, this statement is likely to be approximately true even if a larger family of area distributions is considered than the one taken in Fig. 1.)

When the area distribution V is applied to a plan-form which is narrow near the apex, the ratio between the local thickness and the local span becomes rather large there. This property may be undesirable (the ratio between the usable and the total volume may be too small and the cross section shapes might be detrimental to the development of the leading edge vortices at incidence). The minimum K_0 values for fixed $S''(1)$ and various values of $S''(0)$ plotted in Fig. 2 suggest that it should be possible to modify the area distribution V (for which $S''(0) = 56$) and reduce the area near the apex of the wing without increasing K_0 a great deal.

3. *The Wave Drag of Delta Wings with Rhombic Cross Sections by Non-Slender Thin-Wing Theory.*
 3.1. *The Oblique Cross-Sectional Area Distributions.* Slender-body theory predicts in certain cases implausibly low values of the wave drag. It is therefore essential to investigate the validity of the slenderness assumption for such cases. The application of the full linearised theory which makes neither the slenderness assumption nor the thin-wing assumption is too laborious, therefore we investigate the problem by determining the difference in the wave drags calculated by slender theory and by non-slender thin-wing theory.

We consider a class of wings which is reasonably wide but on the other hand of a sufficiently simple geometry for the calculation of the wave drag by thin-wing theory to be not too lengthy.

We choose wings of delta plan-form with rhombic cross sections and a polynomial expression for the shape of the centre section:

$$z(x, y) = \frac{1}{2s} \left(x - \frac{|y|}{s} \right) (1-x) \sum_{n=0}^N A_n x^n. \quad (20)$$

(As in the previous section: x, y, z is a rectangular co-ordinate system with the x -axis in the free-stream direction, s is the semi-span at the trailing edge and the root chord c_0 is taken as unity.)

The zero-lift wave drag according to thin-wing theory is given by the relation (see for example Ref. 7):

$$\frac{D}{q} = \frac{2}{\pi} \int_0^{\pi/2} d\theta \left\{ -\frac{l^2(\beta, \theta)}{2\pi} \int_0^1 \int_0^1 \frac{d^2 \left(\frac{S^*(x, \beta, \theta)}{l^2} \right)}{d \left(\frac{x}{l} \right)^2} \frac{d^2 \left(\frac{S^*(x', \beta, \theta)}{l^2} \right)}{d \left(\frac{x'}{l} \right)^2} \times \right. \\ \left. \times \log \left| \frac{x}{l} - \frac{x'}{l} \right| d \left(\frac{x}{l} \right) d \left(\frac{x'}{l} \right) \right\}. \quad (21)$$

For given β and θ , $S^*(x, \beta, \theta)$ is the projection into the plane $x = \text{constant}$ of the cross-sectional area intercepted by the plane through the point $(x, 0, 0)$ which is normal to the median plane of the wing and which makes with the free stream direction the angle $\cot^{-1} \beta \cos \theta$ (see Fig. 4). $l(\beta, \theta)$ is the interval of x over which the cross-sectional area is non-zero:

$$l = l(\beta, \theta) = 1 + b \quad (22)$$

with

$$b = \beta s \cos \theta. \quad (23)$$

Instead of x we use the co-ordinate

$$\xi = \frac{x}{l(\beta, \theta)} = \frac{x}{1+b} \quad (24)$$

and

$$S(\xi, \beta, \theta) = \frac{S^*[x = \xi(1+b), \beta, \theta]}{l^2(\beta, \theta)}. \quad (25)$$

To determine $S(\xi, \beta, \theta)$ for given β and θ we integrate the local wing thickness along the straight line

$$y' = \frac{x - x'}{\beta \cos \theta} = s \frac{x - x'}{b}.$$

The projection of this area into a plane normal to the x -axis is then given by:

$$S^*(x, \beta, \theta) = 2 \int_{y_2}^{y_1} z(x', y') dy' \\ = -2 \int_{x_1}^{x_2} z(x', y') \frac{dy'}{dx'} dx' \\ = \frac{2s}{b} \int_{x_1}^{x_2} z(x', y') dx'. \quad (26)$$

For the co-ordinate ξ the limits of the integral are

$$\begin{aligned} 0 < \xi < \frac{1-b}{1+b} & : & x_1 &= \xi, \\ & & x_2 &= \frac{1+b}{1-b} \xi, \\ \frac{1-b}{1+b} < \xi < 1 & : & x_1 &= \xi, \\ & & x_2 &= 1. \end{aligned}$$

Inserting Equation (20) into Equation (26) and relating the area to $l^2(\beta, \theta)$, we obtain the relations:

$$0 < \xi < \frac{1-b}{1+b} :$$

$$\begin{aligned} S(\xi, \beta, \theta) &= \frac{1}{b^2(1+b)} \int_{\xi}^{(1+b)\xi} \left\{ (x' - \xi)(1-x') \sum_{n=0}^N A_n x'^n \right\} dx' \\ &+ \frac{1}{b^2(1+b)} \int_{(1+b)\xi}^{\frac{1+b}{1-b}\xi} \left\{ \left(\xi - \frac{1-b}{1+b} x' \right) (1-x') \sum_{n=0}^N A_n x'^n \right\} dx' \\ &= \frac{1}{b^2(1+b)} \sum_{n=0}^N A_n \left\{ \xi^{n+2} \frac{(1-b)^{n+1} + (1+b)^{n+1} - 2(1-b^2)^{n+1}}{(1-b)^{n+1} (n+1)(n+2)} \right. \\ &\quad \left. - \xi^{n+3} \frac{(1-b)^{n+2} + (1+b)^{n+2} - 2(1-b^2)^{n+2}}{(1-b)^{n+2} (n+2)(n+3)} \right\}, \end{aligned}$$

$$\frac{1-b}{1+b} < \xi < \frac{1}{1+b} :$$

$$\begin{aligned} S(\xi, \beta, \theta) &= \frac{1}{b^2(1+b)} \sum_{n=0}^N A_n \left\{ -\frac{1-b}{1+b} \frac{1}{(n+2)(n+3)} \right. \\ &+ \xi \frac{1}{(n+1)(n+2)} - \xi^{n+2} \frac{2(1+b)^{n+1} - 1}{(n+1)(n+2)} \\ &\quad \left. + \xi^{n+3} \frac{2(1+b)^{n+2} - 1}{(n+2)(n+3)} \right\}, \end{aligned}$$

$$\frac{1}{1+b} < \xi < 1:$$

$$\begin{aligned} S(\xi, \beta, \theta) &= \frac{1}{b^2(1+b)} \sum_{n=0}^N A_n \left\{ \frac{1}{(n+2)(n+3)} \right. \\ &\quad \left. - \xi \frac{1}{(n+1)(n+2)} + \xi^{n+2} \frac{1}{(n+1)(n+2)} \right. \\ &\quad \left. - \xi^{n+3} \frac{1}{(n+1)(n+3)} \right\}. \end{aligned} \tag{27}$$

3.2. *The Numerical Calculation of the Drag.* The next step in the calculation of the drag is the evaluation of the double integral

$$F(b) = -\frac{1}{2\pi} \int_0^1 \int_0^1 S''(\xi, \beta, \theta) S''(\xi', \beta, \theta) \log |\xi - \xi'| d\xi d\xi' \tag{28}$$

Equation (27) shows that in the relations for the area distribution $S(\xi, \beta, \theta)$ the span s , the parameter β and the angle θ do not occur separately but only as the product $b = \beta s \cos \theta$. The same is therefore true for the double integral.

The analytical expression for the second derivative of $S(\xi, \beta, \theta)$ with respect to ξ is given by three different polynomials for the three different intervals of ξ , as in Equation (27). To use these functions for $S''(\xi, \beta, \theta)$ and determine $F(b)$ analytically would lead to extremely lengthy expressions. We have, therefore, refrained from deriving an explicit formula for $F(b)$ and have instead applied the numerical method of Eminton⁴ (see Ref. 3) to obtain approximate values of $F(b)$ for numerically given values of $S(\xi, \beta, \theta)$.

Eminton's method can be applied to determine $F(b)$ for $b \neq 0$ (i.e., $\theta \neq 90$ deg), since for $\theta \neq 90$ deg the area distributions $S(\xi, \beta, \theta)$ satisfy the condition $S'(\xi = 1, \beta, \theta) = 0$ for which the method has been developed.

The values of $F(b)$ are finite for $\theta \neq 90$ deg but if $S'(\xi = 1, \beta, \theta = 90 \text{ deg}) \neq 0$, then $F(b)$ tends to infinity when θ tends to 90 deg. It is shown in the Appendix that F tends to infinity as $-1/2\pi[S'(1)]^2 \log \cos \theta$, where $S'(1)$ is the streamwise derivative at the trailing edge of the cross-sectional area distribution in planes normal to the stream.

We therefore write Equation (21) for the drag in the form:

$$\begin{aligned} \frac{D}{q} &= \frac{2}{\pi} \int_0^{\pi/2} \left\{ l^2(\beta, \theta) F(\beta s \cos \theta) + \frac{[S'(1)]^2}{2\pi} \log \cos \theta \right\} d\theta \\ &\quad - \frac{[S'(1)]^2}{2\pi} \frac{2}{\pi} \int_0^{\pi/2} \log \cos \theta d\theta \\ &= \frac{2}{\pi} \int_0^{\pi/2} \left\{ l^2(\beta, \theta) F(\beta s \cos \theta) + \frac{[S'(1)]^2}{2\pi} \log \cos \theta \right\} d\theta \\ &\quad + \frac{[S'(1)]^2}{2\pi} \log 2, \end{aligned} \quad (29)$$

using the relation

$$\int_0^{\pi/2} \log \cos \theta d\theta = -\frac{\pi}{2} \log 2.$$

The integrand in Relation (29) is finite over the whole θ range ($l(\beta, \theta) \rightarrow 1$ for $\theta \rightarrow 90$ deg). Therefore the integration with respect to θ can be performed numerically or graphically.

For the numerical calculations, we have considered wings with $N = 3$ in Equation (20) for the thickness distribution. $N = 3$ has been chosen to allow an independent choice of the three parameters $S''(0)/v$, $S'(1)/v$ and $S''(1)/v$, which have been considered in the previous section. The drag of any arbitrary thickness distribution with $N = 3$ for given value of the parameter βs can be written in the form:

$$\frac{D(\beta s)}{q} = \sum_{\nu=0}^3 \sum_{\mu=0}^3 F_{\nu\mu}(\beta s) A_\nu A_\mu. \quad (30)$$

Since the drag is a function of the product βs only and not of β and s separately, the coefficients $F_{\nu\mu}$ depend on βs only. To determine the 10 coefficients $F_{\nu\mu}$ one has to calculate the drag by Equation (29) for at least 10 properly chosen thickness distributions.

The following cases were taken:

$$A_\nu = 1, \quad A_n = 0 \text{ for } n \neq \nu; \quad \nu = 0, 1, 2, 3$$

$$A_{\nu+\mu} = -A_\nu, \quad A_n = 0 \text{ for } n \neq \nu, \quad n \neq \nu + \mu, \quad \nu = 0, 1, 2, \quad \mu = 1, 2, 3, \mu > 0.$$

The area distributions $S(\xi, \beta, \theta)$ have been calculated for $b = \beta s \cos \theta = 0.1, 0.2, \dots, 0.8$ and by using Eminent's programme for the automatic computer DEUCE at the Royal Aircraft Establishment the corresponding functions $F(\beta s \cos \theta)$ were determined numerically and the $D(\beta s)/q$ for $\beta s = 0.2, 0.3 \dots 0.8$ were determined graphically using Equation (29). The results are given in Table 2. The accuracy of the last figure of the quoted results is in doubt since Eminent's programme gives only approximate values of $F(\beta s \cos \theta)$ and since the $D(\beta s)/q$ were determined graphically from the knowledge of the integrand at a relatively small number of θ -values.

From the results of Table 2, the coefficients $F_{\nu\mu}$ in Equation (30) can be calculated. For those cases where $S'(1) \neq 0$, the drag tends to infinity when βs tends to zero. Since it is known that D/q tends to infinity as $-1/2\pi[S'(1)]^2 \log \beta s$, it is convenient to express D/q in the form:

$$\frac{D(\beta s)}{q} = \sum_{\nu=0}^3 \sum_{\mu=0}^3 f_{\nu\mu}(\beta s) A_\nu A_\mu - \frac{1}{2\pi} [S'(1)]^2 \log \beta s \quad (31)$$

The coefficients $f_{\nu\mu}$ are finite for all βs and can be calculated from:

$$f_{\nu\mu}(\beta s) = F_{\nu\mu}(\beta s) + \frac{\log \beta s}{2\pi}$$

since

$$-S'(1) = \sum_{n=0}^3 A_n.$$

The $f_{\nu\mu}$ are tabulated in Table 3.

3.3. Comparison of the Drag Coefficients Calculated by Thin-Wing Theory and by Slender-Body Theory. As a first application of the coefficients given in Table 3, Figs. 5 to 7 show the drag factors K_0 for wings I, II and V of Refs. 5 and 6, for which the drag and pressure distributions are being determined experimentally in the 8 ft tunnel at R.A.E. Bedford. In Figs. 5 to 7 the drag factors from thin-wing theory are plotted together with those from slender-body theory. We notice that the differences between the results from the two theories are of different character for the three wings. For wing V the differences are small up to large values of the slenderness parameter βs . The differences for wing II are of different sign from those for wings I and V.

As a further example for the differences in the drag factors calculated by the two methods, Fig. 8 shows the ratio between the drag values from the two theories for the ten wings, for which the thin-wing theory drag values have been calculated originally. To simplify the discussion of the results, we have quoted in Fig. 8 the values of the first and second derivatives of the area distribution at the apex and at the trailing edge for unit volume of the wing. We notice that for the wings with $S'(1) = 0$, slender-body theory gives larger values for the drag than thin-wing theory. The differences between the results of the two theories are the larger, the larger the value of $S''(1)$. For wings with finite $S'(1)$, slender-body theory produces lower drag values than thin-wing theory,

the differences increase again with increasing values of $|S''(1)|$. Such a dependence of the differences of the results between slender and non-slender theory was to be expected. A large value of $|S''(1)|$ corresponds to a large value of the streamwise curvature of the wing at the trailing edge

$$\left(S''(1) = \frac{z''(x=1, y=0)}{2s} \right),$$

i.e., the wing is not slender near the rear end. The larger the value of $|S''(1)|$ the smaller is the value of βs at which the slenderness assumption becomes first in error by a given amount.

Fig. 8 shows thus that it is not possible to quote a numerical value of the slenderness parameter βs , up to which slender theory is valid (as is sometimes done) without making a statement about the geometry of the configuration considered.

Since the application of slender-body theory is for most of the practical configurations so much simpler than the application of thin-wing theory, it would be desirable to know some estimates for the limits within which slender theory can be used. For slender aircraft the area distribution varies in most cases rather slowly in the streamwise direction, so that it seems sufficient, for a first crude investigation, to consider the first and second derivatives of the area distribution at apex and trailing edge as characteristic parameters.

In an attempt to isolate the effect of one parameter, we have plotted in Figs. 9 to 11 the drag factors calculated by the two theories for various area distributions with only one parameter varying in each figure.

Fig. 9 suggests that the validity of the slenderness assumption does not depend much on the value of $S''(0)$, the second derivative of the area distribution at the apex.

Figs. 10 and 11 show that the value of the second derivative at the trailing edge, $-S''(1)$, is more important than the value of the first derivative $-S'(1)$, in determining whether the slenderness assumption is valid for a given configuration.

A quantitative statement about the dependence of the validity of the slenderness assumption on the value of $S''(1)$ and on βs is given in Fig. 12, where results for various values of $S''(0)$ and $S'(1)$ are plotted together. The figure shows that for fixed values of $S''(1)$ and βs the ratio between the drag values from slender and from non-slender theory decreases with decreasing K_0 calculated by slender theory. Until calculations of the drag factor by thin-wing theory have been made for more general thickness distributions, *i.e.*, for wings of other than delta plan-form, of other than rhombic cross-sections, and for a larger family of centre section shapes than considered here, Fig. 12 may be used as a guide when assessing the applicability of slender theory for a given case.

3.4. *Minimum Drag Values.* A further interesting question arises, namely: what is the minimum drag value of a delta wing according to thin-wing theory for given βs and for certain fixed properties of the wing? The minimum K_0 plotted in Fig. 13 were obtained by substituting in Equation (31) the constants A_1 , A_2 and A_3 by the volume v , $S'(1)$ and $S''(1)$ and differentiating the resulting equation with respect to A_0 for fixed βs , v , $S'(1)$ and $S''(1)$. The main result of Fig. 13 is that the minimum K_0 for given $S''(1)/v$ varies only slightly with varying $S''(1)/v$ in contrast to the result from slender-body theory, *see* Fig. 1. In a non-slender theory, the drag values calculated by thin-wing theory differ from those calculated without the thin-wing assumption. It is known from experimental and theoretical evidence that, at least in certain cases, thin-wing theory overestimates the perturbation velocities and thus may overestimate the normal-pressure drag. The results of Fig. 13 may thus be pessimistic for configurations where the thin-wing assumption is not justified.

The minimum K_0 for given values of $S''(0)$ are plotted in Fig. 14, which shows that a variation of $S''(0)$ has the same type of effect as with the results from slender theory in Fig. 2.

Finally, Fig. 15 shows how the minimum K_0 varies with the slenderness parameter βs .

Figs. 13 and 14 suggest that the drag of the area distribution V ($S''(0)/v = 56$, $-S'(1)/v = 7$, $-S''(1)/v = 14$, $K_0(\beta s = 0.4) = 0.78$) cannot be reduced much by increasing $-S''(1)/v$ as was suggested by the results from slender theory. There exist on the other hand area distributions which have about the same drag as the area distribution V, but have lower values of $S''(0)/v$ and larger values of $-S'(1)/v$ (together with a properly chosen $S''(1)$) which are required in certain practical cases.

4. *Conclusions.* 4.1. Calculations according to slender-body theory have shown that, for area distributions given by polynomials and for given value of the slenderness parameter βs ,

- (a) a minimum value of the zero-lift wave drag factor K_0 exists if the second derivative of the area distribution at the trailing edge, $S''(1)$, is fixed;
- (b) the minimum value of K_0 decreases with increasing $-S''(1)$.

4.2. Calculations according to non-slender thin-wing theory have shown that, for given βs ,

- (a) a minimum of K_0 exists (at least for delta wings with rhombic cross sections and centre sections which are polynomials of 5th degree);
- (b) the minimum value of K_0 does not vary much with the value of $S''(1)$.

4.3. Comparison of the K_0 values from slender theory with those from thin-wing theory have shown that the error in the K_0 estimate due to the slenderness assumption depends mainly on the values of $S''(1)$ and $K_{0\text{SLENDER}}$ but not on $S''(0)$ and $S'(1)$.

4.4. Both theories suggest the existence of area distributions with less area near the apex and more area near the trailing edge compared to the Lord V area distribution (as required in practical cases) which have no larger K_0 than the area distribution V.

NOTATION

b	=	$\beta s \cos \theta$
c_0	=	1, wing chord at centre section
D		Normal pressure drag
$F(b)$		<i>See</i> Equation (28)
k		<i>See</i> Equations (1) and (2)
K_0	=	$(D/qv^2)(\pi/128)$ zero-lift wave drag factor, ratio between the drag of the given configuration and the drag of the Sears-Haack body of the same length and volume
$l(\beta, \theta)$	=	$1 + b$, streamwise distance over which the area $S^*(x, \beta, \theta)$ is not zero, <i>see</i> Fig. 4
M_0		Free-stream Mach number
q		Dynamic pressure of free-stream
s		Semi-span at the trailing edge
$S(x)$		Cross-sectional area in plane normal to the free-stream
$S'(x), S''(x)$		First and second derivative of $S(x)$ with respect to x
$S^*(x, \beta, \theta)$		Projection into the plane $x = \text{constant}$ of the cross-sectional area intercepted by the plane through the point $(x, 0, 0)$ which is normal to the median plane of the wing and makes with the free-stream direction the angle $\cot^{-1} \beta \cos \theta$
$S(\xi, \beta, \theta)$	=	$\frac{S^*(x = \xi(1+b), \beta, \theta)}{l^2(\beta, \theta)}$
v		Volume of the wing
x, y, z		Cartesian co-ordinates with the origin at the apex of the wing; the x -axis measured in the direction of the undisturbed stream; the z -axis normal to the chordal plane of the wing
β	=	$\sqrt{(M_0^2 - 1)}$
ξ	=	$x/(1+b)$
η	=	y/s

REFERENCES

- | <i>No.</i> | <i>Author</i> | <i>Title, etc.</i> |
|------------|-----------------------------------|---|
| 1 | M. J. Lighthill | The wave drag at zero-lift of slender delta wings and similar configurations.
<i>J. Fluid Mech.</i> Vol. 1. Part 3, p. 337. September, 1956. |
| 2 | J. H. Willis and D. G. Randall .. | The theoretical wave drag of open-nose axisymmetrical forebodies with varying fineness ratio, area ratio and nose angle.
C.P. 245. February, 1955. |
| 3 | J. Weber | Numerical methods for calculating the zero-lift wave drag and the lift-dependent wave drag of slender wings.
R. & M. 3221. December, 1959. |
| 4 | E. Eminton | On the minimisation and numerical evaluation of wave drag.
A.R.C. 19,212. November, 1955. |
| 5 | J. Weber | Slender delta wings with sharp edges at zero lift.
A.R.C. 19,549. May, 1957. |
| 6 | W. T. Lord and G. G. Brebner .. | Supersonic flow past slender pointed wings with 'similar' cross sections at zero lift.
<i>Aero. Quart.</i> Vol. 10, p. 79. February, 1959. |
| 7 | H. Lomax | The wave drag of arbitrary configurations in linearized flow as determined by areas and forces in oblique planes.
N.A.C.A./TIB/4620. March, 1955. |

APPENDIX

The Behaviour of $F(b) = -\frac{1}{2\pi} \int_0^1 \int_0^1 S''(\xi, \beta, \theta) S''(\xi', \beta, \theta) \log |\xi - \xi'| d\xi d\xi'$ For Small Values of $b = \beta s \cos \theta$. To investigate the behaviour of $F(b)$ for small values of b , we split the double integral into three terms:

$$\begin{aligned}
 & -\frac{1}{2\pi} \int_0^1 \int_0^1 S''(\xi, \beta, \theta) S''(\xi', \beta, \theta) \log |\xi - \xi'| d\xi d\xi' = \\
 & -\frac{1}{2\pi} \int_0^{\frac{1-b}{1+b}} \int_0^{\frac{1-b}{1+b}} S''(\xi, \beta, \theta) S''(\xi', \beta, \theta) \log |\xi - \xi'| d\xi d\xi' \\
 & -\frac{1}{\pi} \int_0^{\frac{1-b}{1+b}} \left[S''(\xi, \beta, \theta) \int_{\frac{1-b}{1+b}}^1 S''(\xi', \beta, \theta) \log (\xi' - \xi) d\xi' \right] d\xi \\
 & -\frac{1}{2\pi} \int_{\frac{1-b}{1+b}}^1 \int_{\frac{1-b}{1+b}}^1 S''(\xi, \beta, \theta) S''(\xi', \beta, \theta) \log |\xi - \xi'| d\xi d\xi' \tag{32}
 \end{aligned}$$

We shall see later that it is sufficient to consider thickness distributions which near the trailing edge are of the form

$$z(x, y) = \frac{1}{2s} \left[C(1-x) + D(1-x)^2 \right] \left(x - \frac{|y|}{s} \right) \tag{33}$$

This thickness distribution produces in the interval $\frac{1-b}{1+b} < \xi < 1$ the area distribution:

$$\begin{aligned}
 S(\xi, \beta, \theta) &= \frac{1}{(1+b)^2} \int_{\frac{\xi(1+b)-1}{b}}^{\xi} \left\{ C \left[1 - \xi(1+b) + b \frac{y'}{s} \right] \right. \\
 & \quad \left. + D \left[1 - \xi(1+b) + b \frac{y'}{s} \right]^2 \right\} \times \\
 & \quad \times \left\{ \xi(1+b) - b \frac{y'}{s} - \frac{|y'|}{s} \right\} d \frac{y'}{s} \tag{34}
 \end{aligned}$$

The second derivative of this reads:

$$\begin{aligned}
 S''(\xi, \beta, \theta) &= C \left\{ \frac{\xi(2+b) - 1}{b(1+b)} - \frac{|\xi(1+b) - 1|}{b^2} \right\} \\
 & \quad - D \left\{ \frac{\xi^2(3 + 3b + b^2) - \xi 2(2+b) + 1}{b(1+b)} \right. \\
 & \quad \left. - \frac{[\xi(1+b) - 1] |\xi(1+b) - 1|}{b^2} \right\} \tag{35}
 \end{aligned}$$

With

$$\eta = \frac{y}{s} = \frac{\xi(1+b) - 1}{b}$$

the third integral in Equation (32) becomes:

$$\begin{aligned} & \int_{\frac{1-b}{1+b}}^1 \int_{\frac{1-b}{1+b}}^1 S''(\xi, \beta, \theta) S''(\xi', \beta, \theta) \log |\xi - \xi'| d\xi d\xi' = \\ & \frac{1}{(1+b)^2} \int_{-1}^{+1} \int_{-1}^{+1} \left[C \left\{ \frac{1 + b(2+b)\eta}{(1+b)^2} - |\eta| \right\} \right. \\ & \quad \left. + Db \left\{ \frac{1 - 2\eta - (3+3b+b^2)b\eta^2}{(1+b)^3} + \eta |\eta| \right\} \right] \times \\ & \quad \times \left[C \left\{ \frac{1 + b(2+b)\eta'}{(1+b)^2} - |\eta'| \right\} \right. \\ & \quad \left. + Db \left\{ \frac{1 - 2\eta' - (3+3b+b^2)b\eta'^2}{(1+b)^3} + \eta' |\eta'| \right\} \right] \times \\ & \quad \times \log \frac{b|\eta - \eta'|}{1+b} d\eta d\eta' \\ & = C^2 \int_{-1}^{+1} \int_{-1}^{+1} \{1 - |\eta|\} \{1 - |\eta'|\} \log |\eta - \eta'| d\eta d\eta' \\ & \quad + C^2 \log b \left[\int_{-1}^{+1} \{1 - |\eta|\} d\eta \right]^2 \\ & \quad + \text{term of order } b \text{ and term of order } b \log b. \end{aligned}$$

It follows from Equation (34) that

$$\begin{aligned} S'(\xi, \beta, \theta) &= \frac{1}{1+b} \int_{\frac{\xi(1+b)-1}{b}}^{\xi} \left\{ C \left[1 - 2\xi(1+b) + 2b \frac{y'}{s} + \frac{|y'|}{s} \right] \right. \\ & \quad \left. + D \left[1 - 3\xi(1+b) + 3b \frac{y'}{s} + 2 \frac{|y'|}{s} \right] \right\} \times \\ & \quad \times \left[1 - \xi(1+b) + b \frac{y'}{s} \right] d \left(\frac{y'}{s} \right) \end{aligned}$$

and

$$\begin{aligned} S' \left(\xi = \frac{1-b}{1+b}, \beta, \theta \right) &= -C \int_{-1}^{+1} \left[1 - \frac{|y'|}{s} \right] d \frac{y'}{s} + \text{term of order } b \\ &= -C + \text{term of order } b. \end{aligned}$$

The streamwise derivative at the trailing edge of the area distribution in sections normal to the free stream $S'(1)$ is equal to $-C$. Thus

$$\begin{aligned}
& \int_{\frac{1-b}{1+b}}^1 \int_{\frac{1-b}{1+b}}^1 S''(\xi, \beta, \theta) S''(\xi', \beta, \theta) \log |\xi - \xi'| d\xi' d\xi = \\
& [S'(1)]^2 \left\{ \log b + \frac{\int_{-1}^{+1} \int_{-1}^{+1} (1 - |\eta|)(1 - |\eta'|) \log |\eta - \eta'| d\eta d\eta'}{\left[\int_{-1}^{+1} (1 - |\eta|) d\eta \right]^2} \right\} \\
& \quad + \text{term of order } b \text{ and term of order } b \log b \\
& = [S'(1)]^2 \{ \log b + \log 2 - k \} \\
& \quad + \text{term of order } b \text{ and term of order } b \log b \text{ with } k \text{ from Equation (2)}.
\end{aligned} \tag{36}$$

If we insert the values of $S''(\xi', \beta, \theta)$ from Equation (35) into the second integral of Equation (32) and perform the integration over ξ' explicitly, we find:

$$\begin{aligned}
& \int_0^{\frac{1-b}{1+b}} \left[S''(\xi, \beta, \theta) \int_{\frac{1-b}{1+b}}^1 S''(\xi', \beta, \theta) \log (\xi' - \xi) d\xi' \right] d\xi = \\
& \quad - S'(1) \int_0^1 S''(x) \log (1-x) dx + \text{term of order } b
\end{aligned} \tag{37}$$

where $S(x)$ is the distribution of the cross-sectional area in planes normal to the free stream.

The value of the first integral in Equation (32) is:

$$\begin{aligned}
& - \frac{1}{2\pi} \int_0^{\frac{1-b}{1+b}} \int_0^{\frac{1-b}{1+b}} S''(\xi, \beta, \theta) S''(\xi', \beta, \theta) \log |\xi - \xi'| d\xi d\xi' = \\
& \quad - \frac{1}{2\pi} \int_0^1 \int_0^1 S''(x) S''(x') \log |x - x'| dx dx' \\
& \quad + \text{term of order } b.
\end{aligned} \tag{38}$$

It follows from the derivation of Equations (36) to (38) that the resulting formulae are not restricted to the thickness distributions of Equation (33) but are applicable to the thickness distributions of Equation (20).

The final result reads:

$$\begin{aligned}
F(b) &= - \frac{1}{2\pi} \int_0^1 \int_0^1 S''(\xi, \beta, \theta) S''(\xi', \beta, \theta) \log |\xi - \xi'| d\xi d\xi' \\
&= - \frac{1}{2\pi} \int_0^1 \int_0^1 S''(x) S''(x') \log |x - x'| dx dx' \\
& \quad + \frac{1}{\pi} S'(1) \int_0^1 S''(x) \log (1-x) dx \\
& \quad - \frac{1}{2\pi} [S'(1)]^2 [\log b + \log 2 - k] \\
& \quad + \text{term of order } b \text{ and term of order } b \log b.
\end{aligned} \tag{39}$$

From the relations:

$$\frac{D}{q} = \frac{2}{\pi} \int_0^{\pi/2} l^2(\beta, \theta) F(\beta s \cos \theta) d\theta$$

$$l(\beta, \theta) = 1 + b$$

$$b = \beta s \cos \theta$$

$$\frac{2}{\pi} \int_0^{\pi/2} \log \cos \theta d\theta = -\log 2$$

we obtain for small values of βs , i.e., small b for all θ :

$$\begin{aligned} \frac{D}{q} = & -\frac{1}{2\pi} \int_0^1 \int_0^1 S''(x)S''(x') \log |x - x'| dx dx' \\ & + \frac{1}{\pi} S'(1) \int_0^1 S''(x) \log(1-x) dx \\ & + \frac{1}{2\pi} [S'(1)]^2 [k - \log \beta s] \\ & + \text{term of order } \beta s \text{ and term of order } \beta s \log \beta s \end{aligned} \quad (40)$$

Equation (40) agrees for $\beta s \rightarrow 0$ with the drag from slender-body theory, Equation (1).

Pressure coefficients calculated by thin-wing theory and by slender-thin-wing theory differ only by terms of order $\beta^2 s^2$ and of order $\beta^2 s^2 \log \beta s$ (see for example Ref. 6). Therefore, the integrated normal-pressure drags calculated by the two theories can also differ only by terms of order $\beta^2 s^2$ and $\beta^2 s^2 \log \beta s$. Thus no terms of order βs or $\beta s \log \beta s$ occur in Equation (40).

TABLE 1

Values of the Integral $-\int_0^1 \int_0^1 x^n x'^m \log |x - x'| dx dx'$

$m \backslash n$	0	1	2	3	4	5	6	7	8	9
0	$\frac{3}{2}$	$\frac{3}{4}$	$\frac{35}{72}$	$\frac{17}{48}$	$\frac{497}{1800}$	$\frac{9}{40}$	$\frac{1483}{7840}$	$\frac{3281}{20160}$	$\frac{32329}{226800}$	$\frac{3191}{25200}$
1	$\frac{3}{4}$	$\frac{7}{16}$	$\frac{11}{36}$	$\frac{67}{288}$	$\frac{14}{75}$	$\frac{149}{960}$	$\frac{292}{2205}$	$\frac{2581}{22400}$	$\frac{2309}{22680}$	$\frac{27541}{302400}$
2	$\frac{35}{72}$	$\frac{11}{36}$	$\frac{2}{9}$	$\frac{25}{144}$	$\frac{1021}{7200}$	$\frac{43}{360}$	$\frac{9077}{88200}$	$\frac{1819}{20160}$	$\frac{21829}{272160}$	$\frac{1817}{25200}$
3	$\frac{17}{48}$	$\frac{67}{288}$	$\frac{25}{144}$	$\frac{53}{384}$	$\frac{137}{1200}$	$\frac{233}{2400}$	$\frac{991}{11760}$	$\frac{5993}{80640}$	$\frac{3011}{45360}$	$\frac{1321}{22050}$
4	$\frac{497}{1800}$	$\frac{14}{75}$	$\frac{1021}{7200}$	$\frac{137}{1200}$	$\frac{143}{1500}$	$\frac{49}{600}$	$\frac{6289}{88200}$	$\frac{2123}{33600}$	$\frac{89951}{1587600}$	$\frac{19393}{378000}$
5	$\frac{9}{40}$	$\frac{149}{960}$	$\frac{43}{360}$	$\frac{233}{2400}$	$\frac{49}{600}$	$\frac{19}{270}$	$\frac{121}{1960}$	$\frac{5167}{94080}$	$\frac{1681}{34020}$	$\frac{18091}{403200}$
6	$\frac{1483}{7840}$	$\frac{292}{2205}$	$\frac{9077}{88200}$	$\frac{991}{11760}$	$\frac{6289}{88200}$	$\frac{121}{1960}$	$\frac{373}{6860}$	$\frac{761}{15680}$	$\frac{111229}{2540160}$	$\frac{7031}{176400}$
7	$\frac{3281}{20160}$	$\frac{2581}{22400}$	$\frac{1819}{20160}$	$\frac{5993}{80640}$	$\frac{2123}{33600}$	$\frac{5167}{94080}$	$\frac{761}{15680}$	$\frac{1557}{35840}$	$\frac{7129}{181440}$	$\frac{65029}{1814400}$
8	$\frac{32329}{226800}$	$\frac{2309}{22680}$	$\frac{21829}{272160}$	$\frac{3011}{45360}$	$\frac{89951}{1587600}$	$\frac{1681}{34020}$	$\frac{111229}{2540160}$	$\frac{7129}{181440}$	$\frac{2423}{68040}$	$\frac{7381}{226800}$
9	$\frac{3191}{25200}$	$\frac{27541}{302400}$	$\frac{1817}{25200}$	$\frac{1321}{22050}$	$\frac{19393}{378000}$	$\frac{18091}{403200}$	$\frac{7031}{176400}$	$\frac{65029}{1814400}$	$\frac{7381}{226800}$	$\frac{7507}{252000}$

Values of the Integral $-\int_0^1 x^m \log(1-x) dx$

m	0	1	2	3	4	5	6	7	8	9
1		$\frac{3}{4}$	$\frac{11}{18}$	$\frac{25}{48}$	$\frac{137}{300}$	$\frac{49}{120}$	$\frac{363}{980}$	$\frac{761}{2240}$	$\frac{7129}{22680}$	$\frac{7381}{25200}$

TABLE 2

$$\frac{D(\beta s)}{q} \text{ or Delta Wings with } z(x, y) = \frac{1}{2s} \left(x - \frac{|y|}{s} \right) (1-x) \sum_{n=0}^3 A_n x^n$$

A_0	A_1	A_2	A_3	$\beta s = 0.2$	0.3	0.4	0.5	0.6	0.7	0.8
1	0	0	0	0.3601	0.3032	0.2658	0.2391	0.2190	0.2039	0.1928
0	1	0	0	0.2587	0.2050	0.1701	0.1452	0.1266	0.1122	0.1007
0	0	1	0	0.2053	0.1560	0.1250	0.1037	0.0882	0.0765	0.0673
0	0	0	1	0.1703	0.1251	0.0978	0.0797	0.0669	0.0575	0.0503
1	-1	0	0	0.0506	0.0491	0.0478	0.0467	0.0459	0.0455	0.0456
1	0	-1	0	0.1168	0.1110	0.1057	0.1013	0.0977	0.0948	0.0930
1	0	0	-1	0.1705	0.1594	0.1495	0.1410	0.1339	0.1282	0.1242
0	1	-1	0	0.01764	0.01627	0.01498	0.01382	0.01281	0.01191	0.01110
0	1	0	-1	0.0488	0.0441	0.0399	0.0362	0.0329	0.0301	0.0277
0	0	1	-1	0.00869	0.00764	0.00672	0.00592	0.00525	0.00470	0.00424

TABLE 3

Coefficients for Calculating the Wave Drag of Delta Wings with

$$z(x, y) = \frac{1}{2s} \left(x - \frac{|y|}{s} \right) (1-x) \sum_{n=0}^3 A_n x^n$$

$$\frac{D(\beta s)}{q} = \sum_{\nu=0}^3 \sum_{\mu=0}^3 f_{\nu\mu}(\beta s) A_\nu A_\mu - \frac{[S'(1)]^2}{2\pi} \log \beta s$$

	$\beta s = 0$		0.2	0.3	0.4	0.5	0.6	0.7	0.8
f_{00}	0.0959		0.1039	0.1116	0.1200	0.1288	0.1377	0.1471	0.1573
f_{11}	-0.0102		0.0025	0.0134	0.0243	0.0349	0.0453	0.0554	0.0652
f_{22}	-0.0699		-0.0509	-0.0356	-0.0208	-0.0066	0.0069	0.0197	0.0318
f_{33}	-0.1124		-0.0859	-0.0665	-0.0480	-0.0306	-0.0144	0.0007	0.0148
$2f_{01}$	0.0326		0.0559	0.0759	0.0964	0.1170	0.1371	0.1571	0.1769
$2f_{02}$	-0.1001		-0.0637	-0.0350	-0.0066	0.0209	0.0469	0.0721	0.0961
$2f_{03}$	-0.2062		-0.1524	-0.1143	-0.0776	-0.0428	-0.0106	0.0197	0.0479
$2f_{12}$	-0.1001		-0.0659	-0.0385	-0.0116	0.0145	0.0394	0.0633	0.0859
$2f_{13}$	-0.1796		-0.1321	-0.0972	-0.0637	-0.0319	-0.0020	0.0261	0.0523
$2f_{23}$	-0.1929		-0.1454	-0.1097	-0.0756	-0.0431	-0.0128	0.0158	0.0424

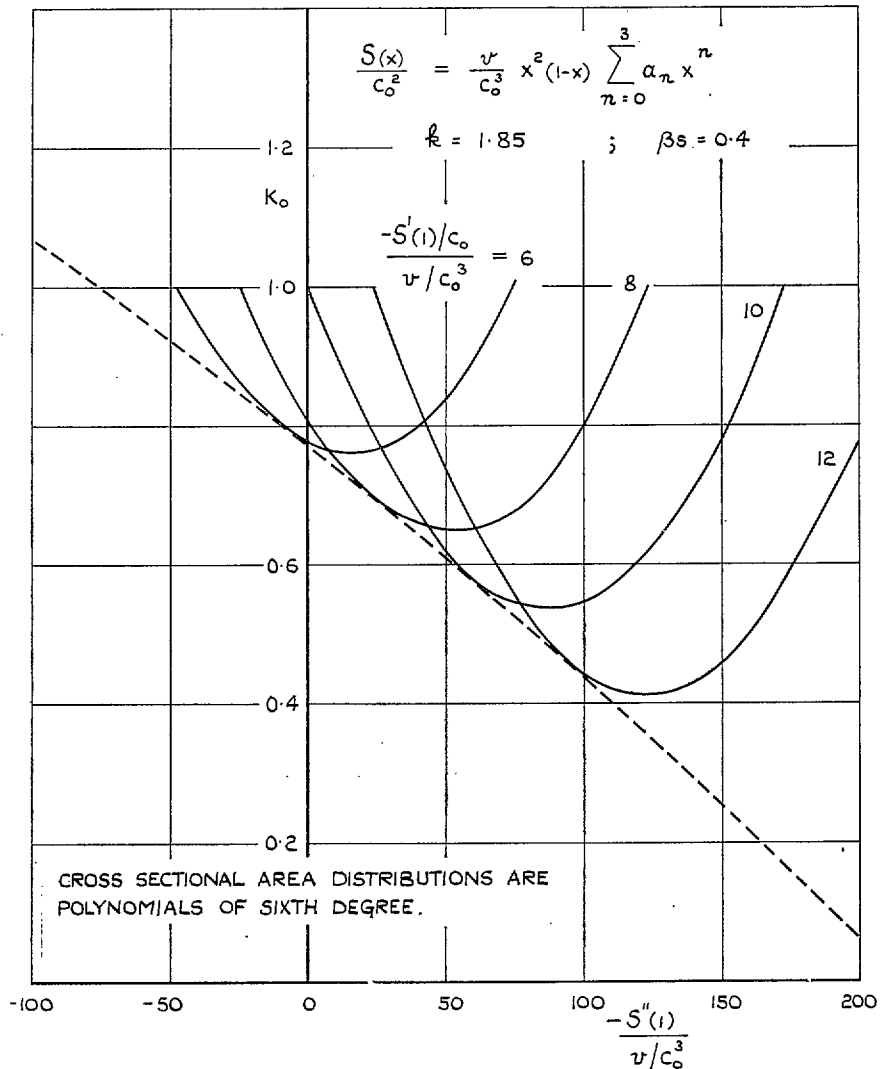


FIG. 1a. Minimum zero-lift drag factors from slender-body theory for given first and second derivatives of the area distribution at the trailing edge.

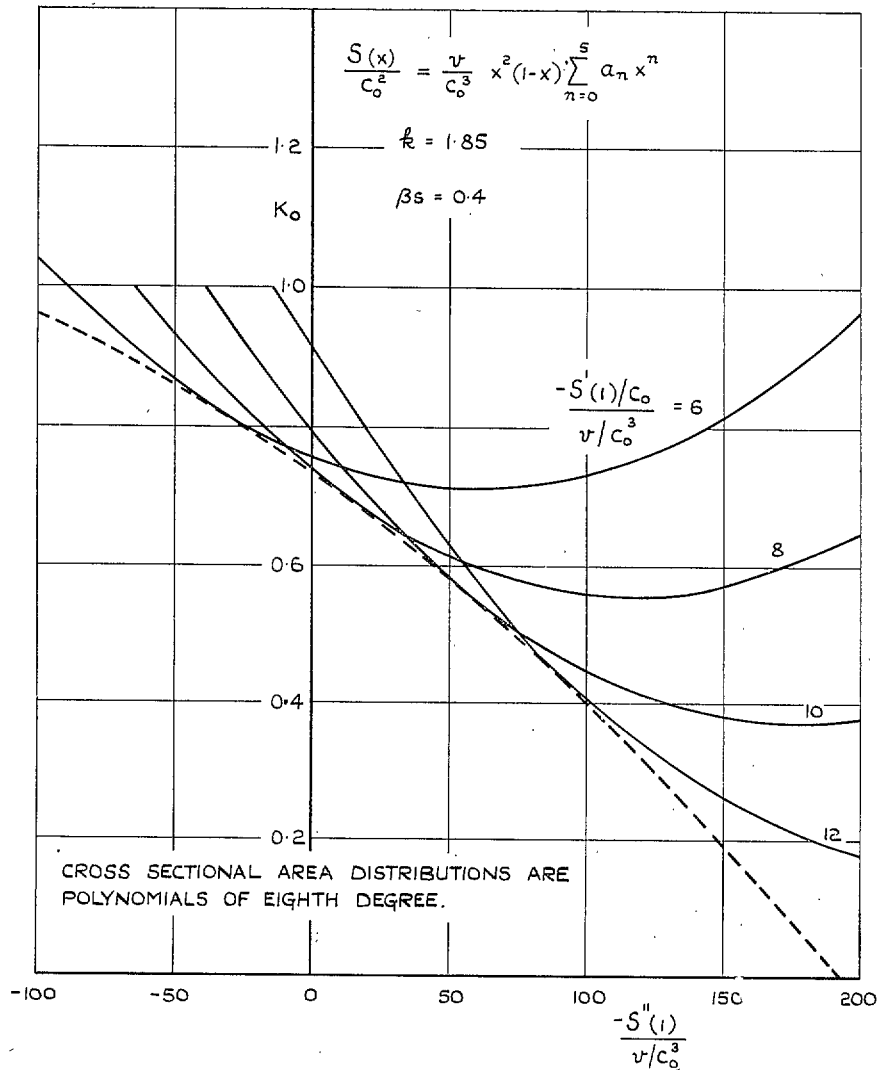


FIG. 1b. Minimum zero-lift drag factors from slender-body theory for given first and second derivatives of the area distribution at the trailing edge.

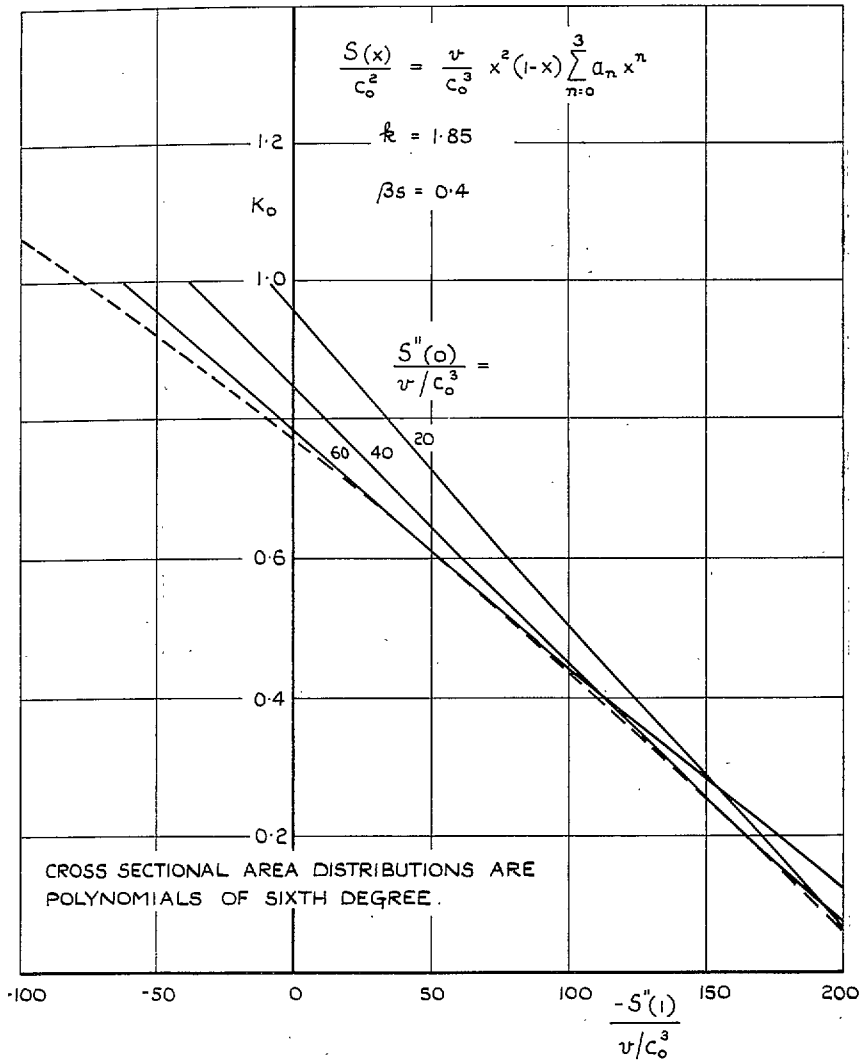


FIG. 2a. Minimum zero-lift drag factors from slender-body theory for given second derivatives of the area distribution at the apex and trailing edge.

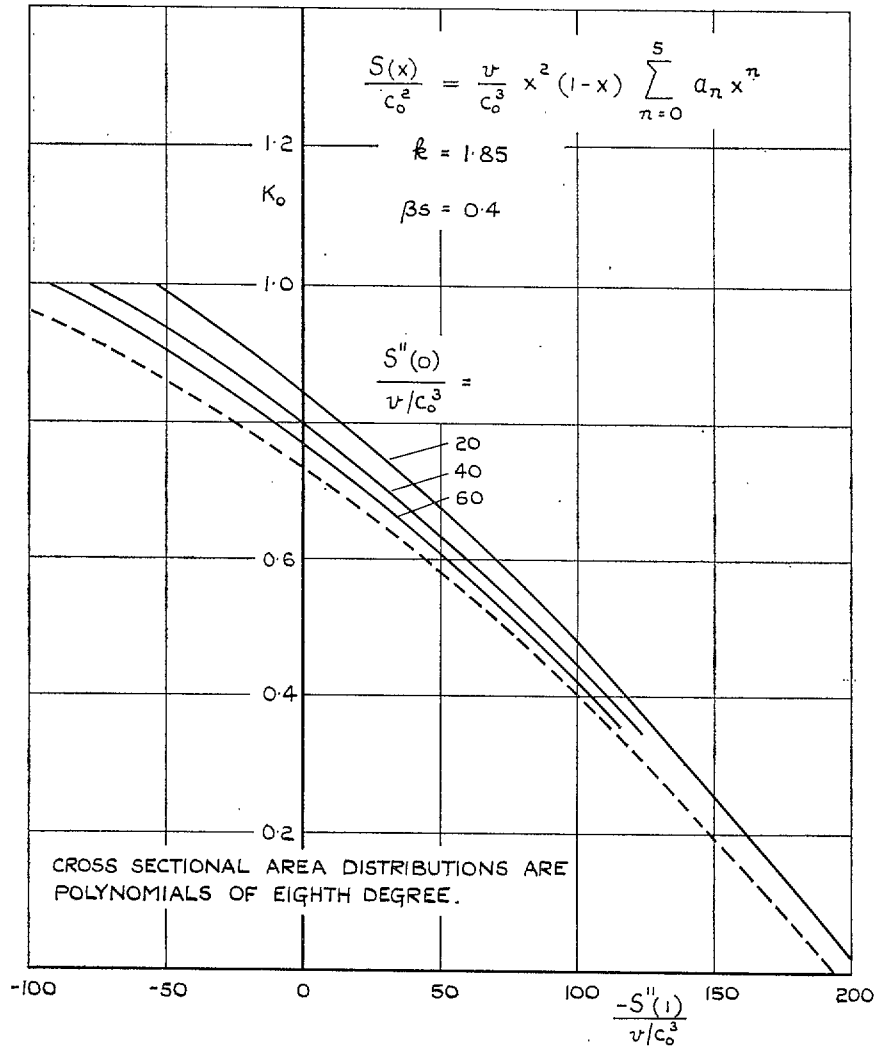


FIG. 2b. Minimum zero-lift drag factors from slender-body theory for given second derivatives of the area distribution at the apex and trailing edge.

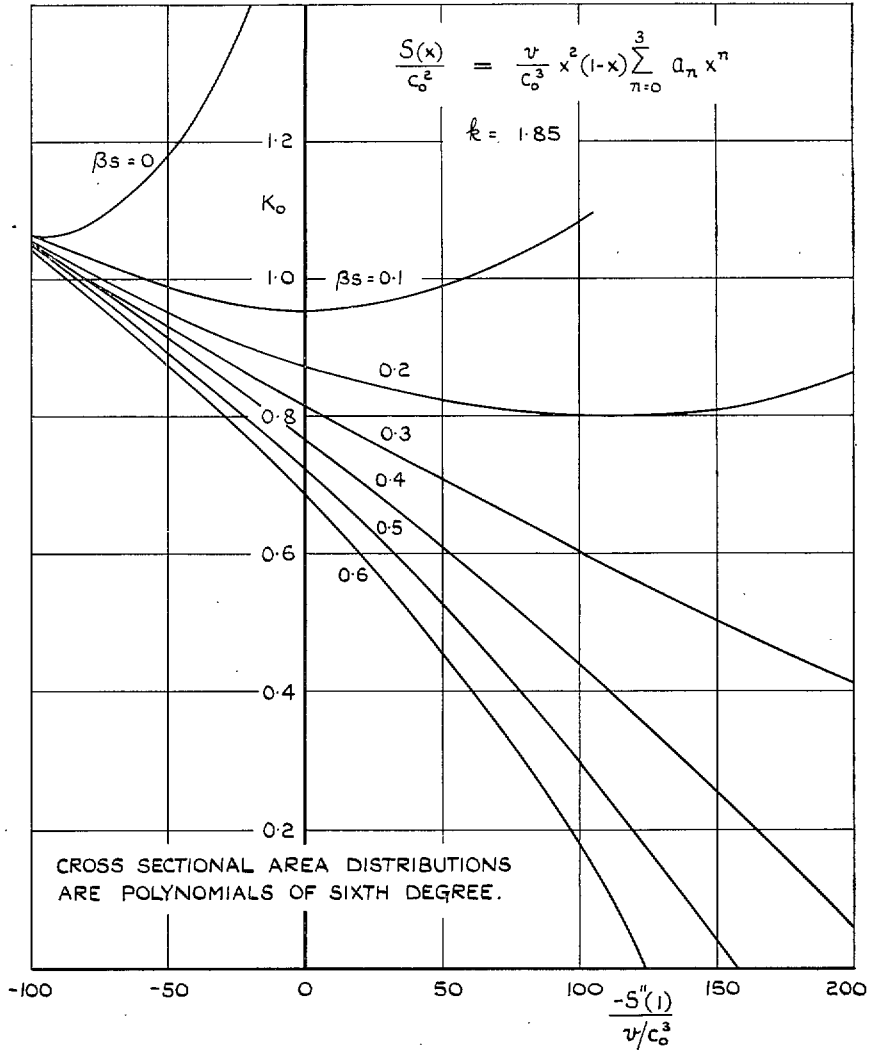


FIG. 3. Minimum zero-lift drag factors from slender-body theory for given second derivative of the area distribution at the trailing edge.

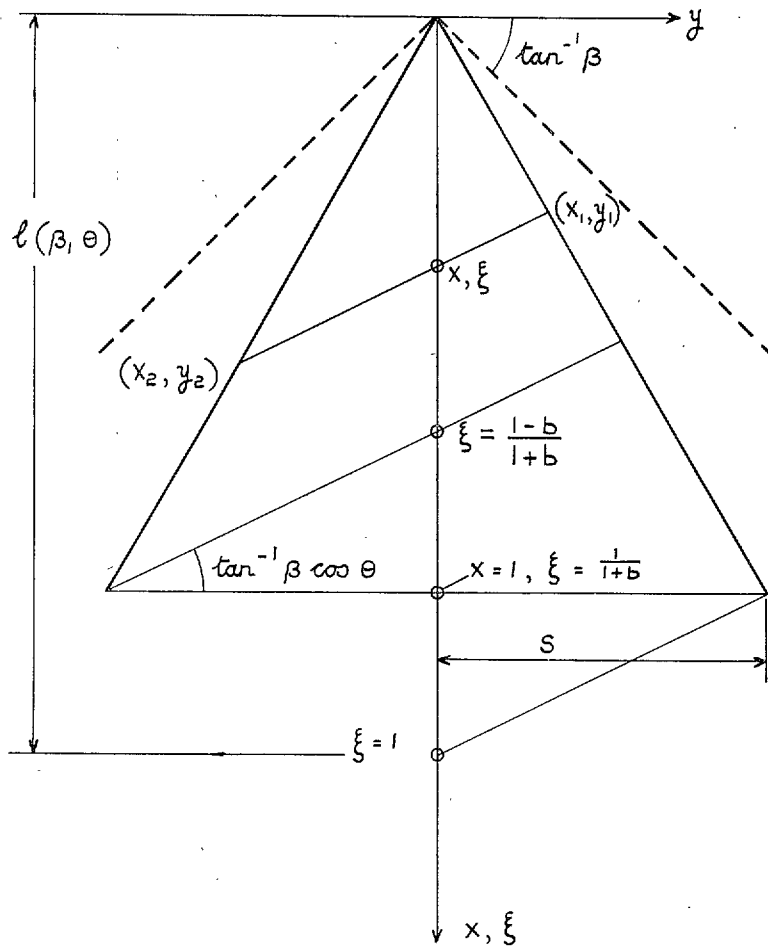


FIG. 4. Notation for Section 3.

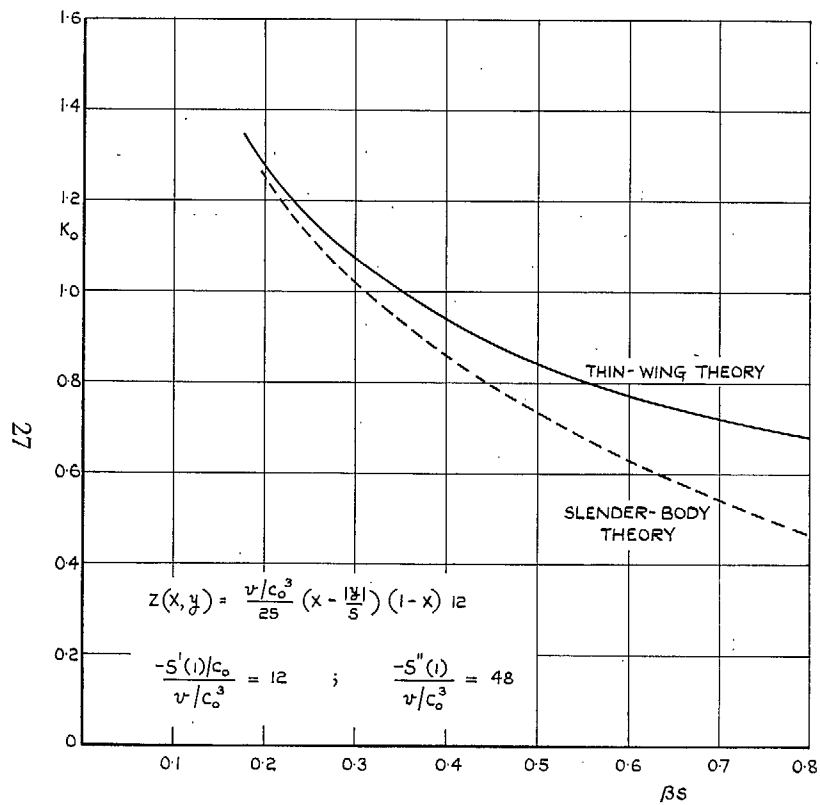


FIG. 5. Zero-lift drag factor for delta wing with biconvex streamwise sections and rhombic cross sections.

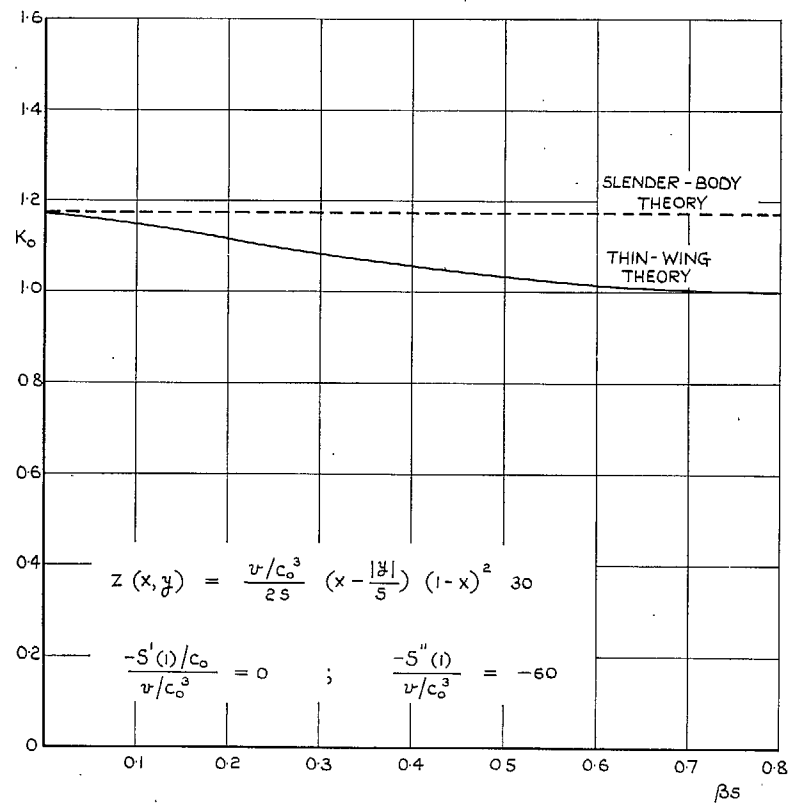


FIG. 6. Zero-lift drag factor for delta wing with rhombic cross sections and area distribution of parabolic body of revolution.

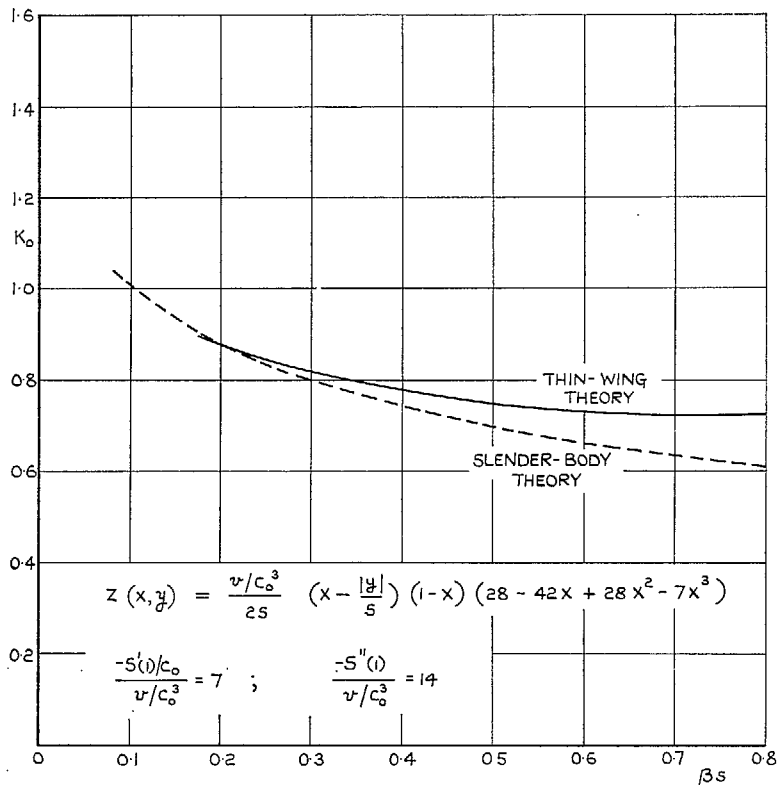
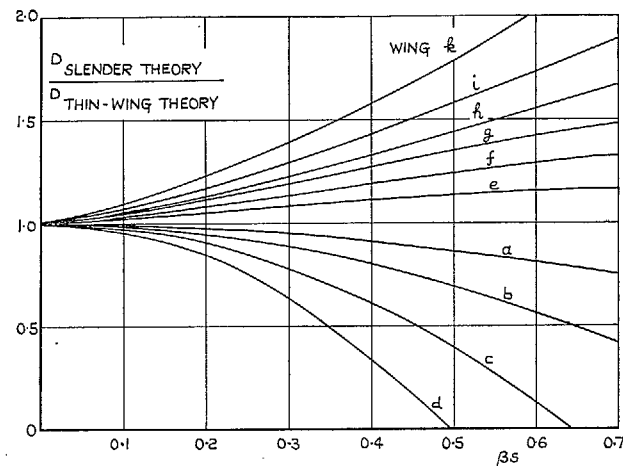


FIG. 7. Zero-lift drag factor for delta wing with rhombic cross sections and Lord V area distribution.



$$z(x,y) = \frac{1}{25} \left(x - \frac{|y|}{5}\right) (1-x) \sum_{n=0}^3 A_n x^n$$

WING	A_0	A_1	A_2	A_3	$\frac{S''(0)}{v/c_0^3}$	$\frac{-S'(l)/c_0}{v/c_0^3}$	$\frac{-S''(l)}{v/c_0^3}$
a	1	0	0	0	24	12	48
b	0	1	0	0	0	20	120
c	0	0	1	0	0	30	240
d	0	0	0	1	0	42	420
e	1	-1	0	0	60	0	-60
f	1	0	-1	0	40	0	-80
g	1	0	0	-1	33.6	0	-100.8
h	0	1	-1	0	0	0	-120
i	0	1	0	-1	0	0	-152.7
k	0	0	1	-1	0	0	-210

FIG. 8. Ratio between drag factors calculated by slender theory and by thin-wing theory for delta wings with rhombic cross sections.

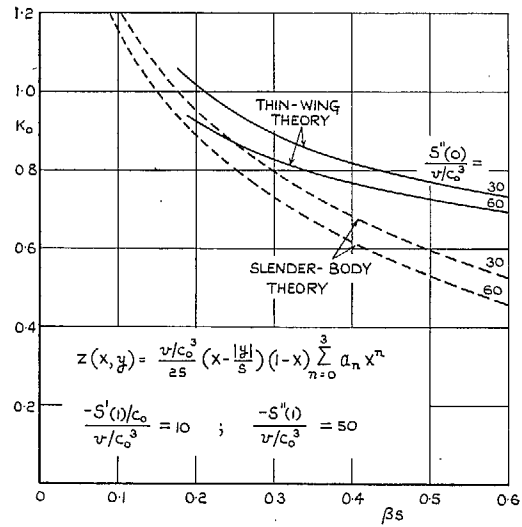


FIG. 9. Zero-lift drag factors for delta wings with different $S''(0)$.

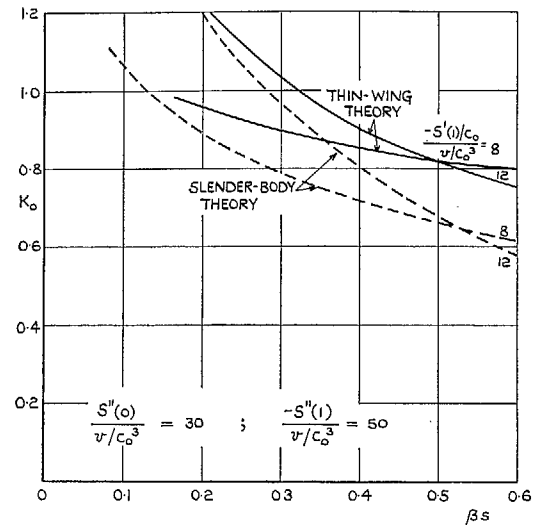
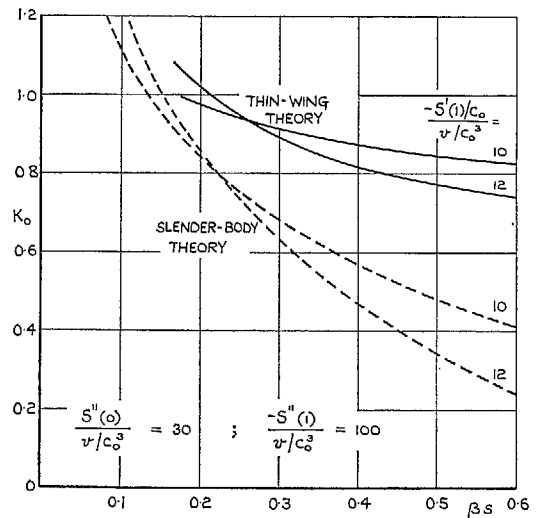
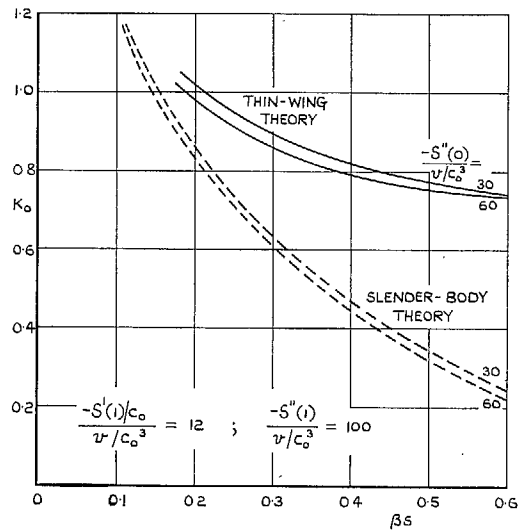


FIG. 10. Zero-lift drag factors for delta wings with different $S'(1)$.



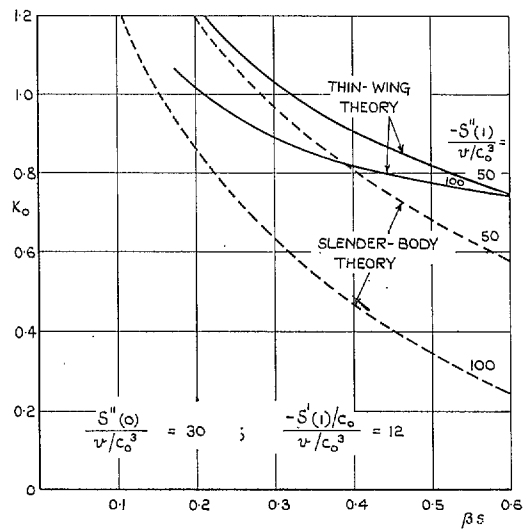
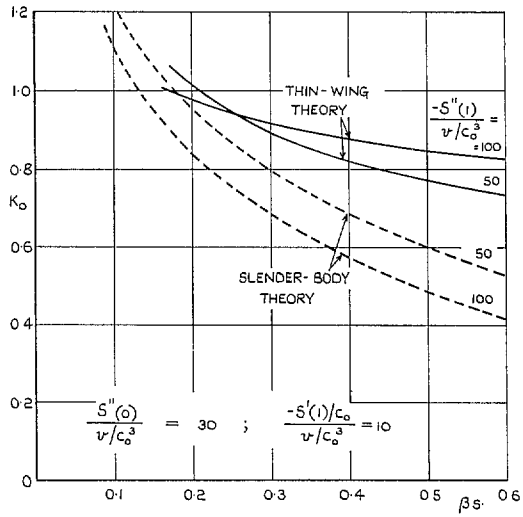


FIG. 11. Zero-lift drag factors for delta wings with different $S''(1)$.

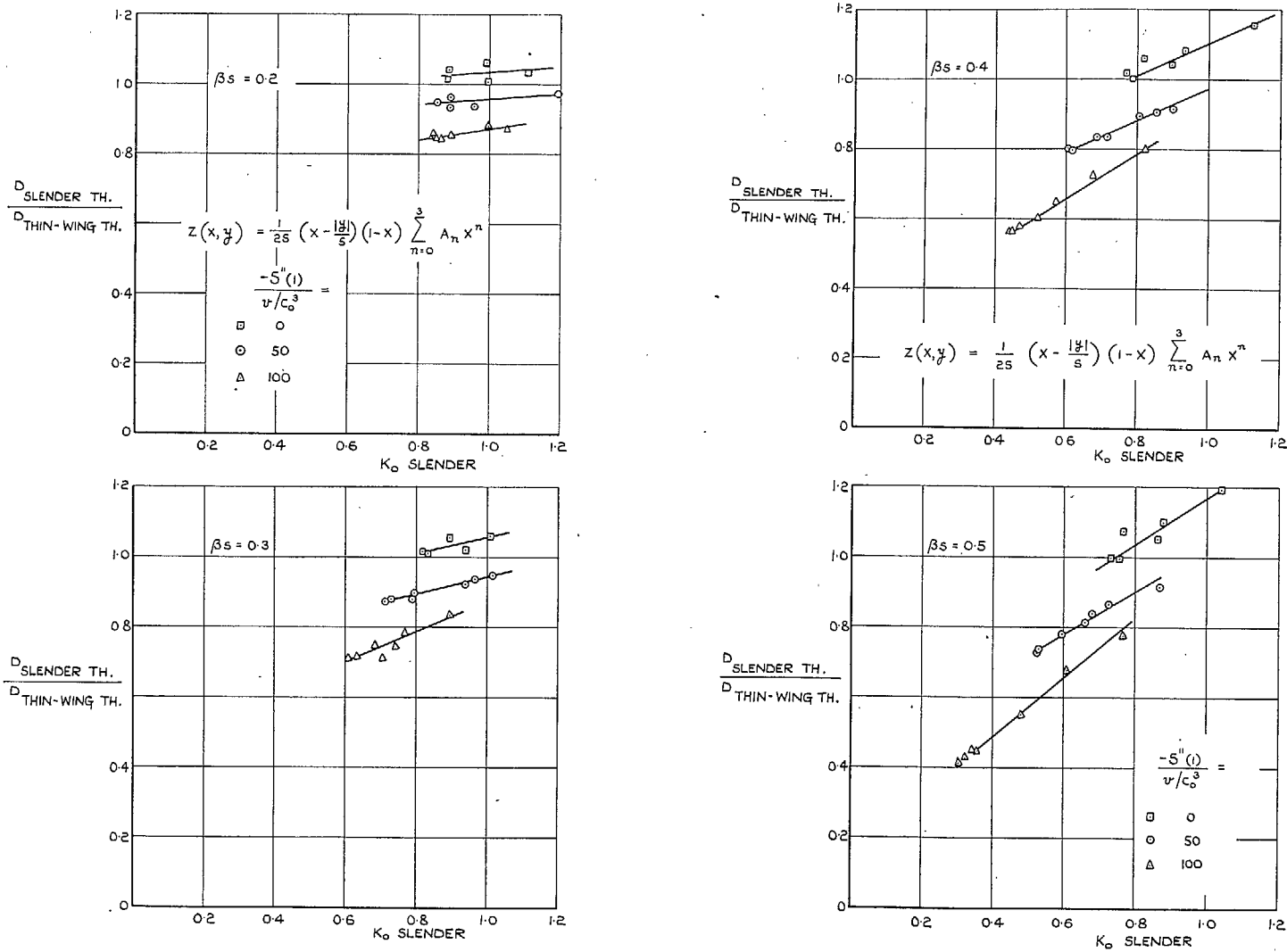


FIG. 12. Ratio between zero-lift wave drag for delta wings calculated by slender-body theory and thin-wing theory.

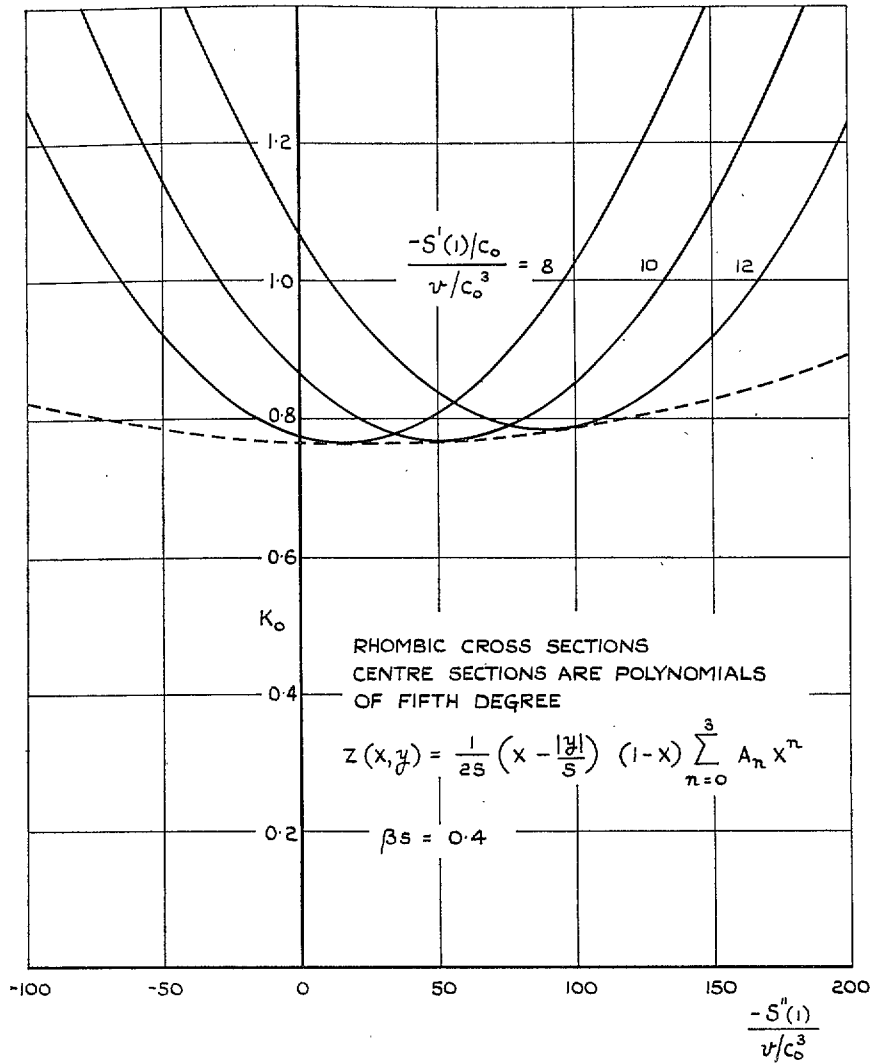


FIG. 13. Minimum zero-lift drag factors from thin-wing theory for delta wings with given first and second derivatives of the area distribution at the trailing edge.

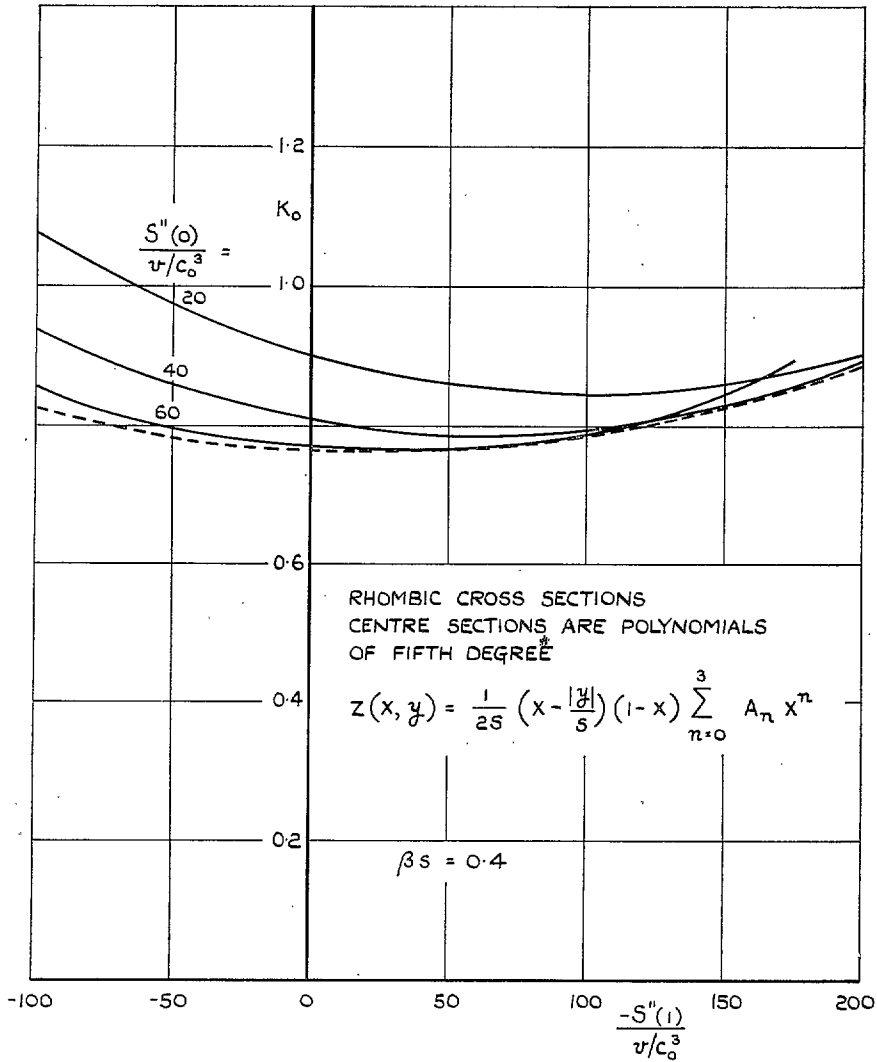


FIG. 14. Minimum zero-lift drag factors from thin-wing theory for delta wings with given second derivatives of the area distribution at the apex and trailing edge.

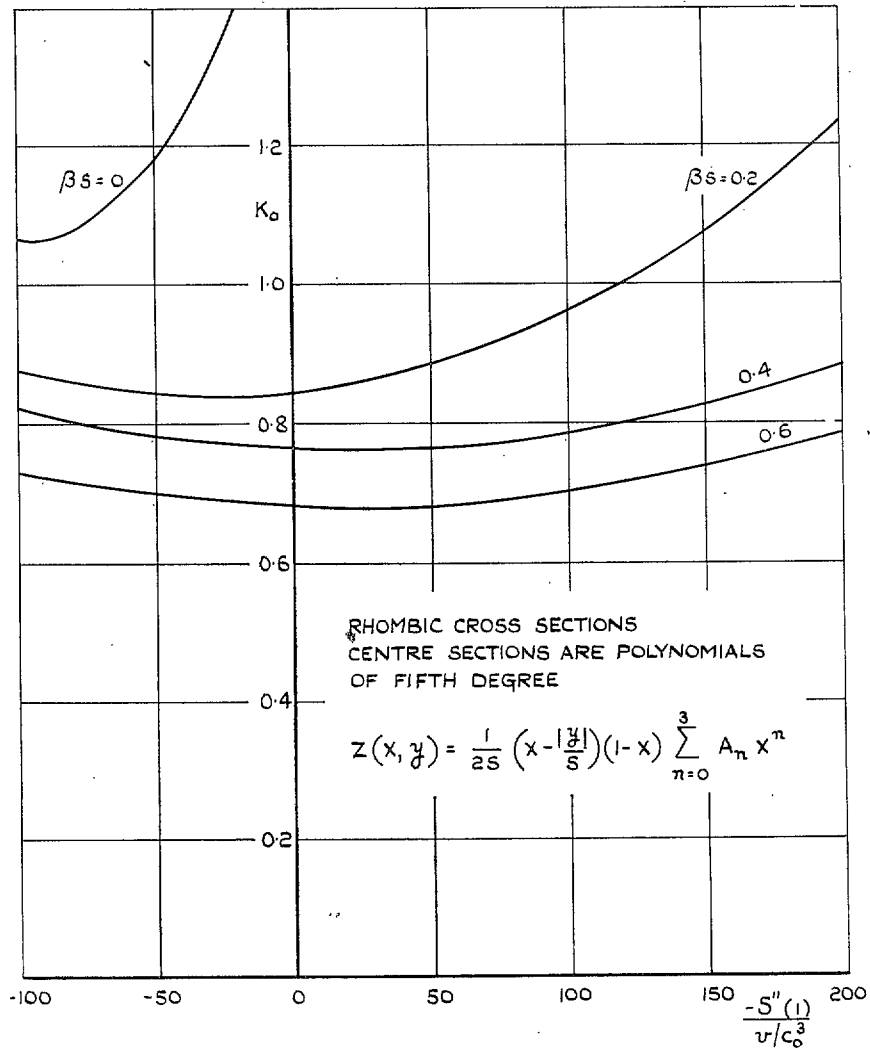


FIG. 15. Minimum zero-lift drag factors from thin-wing theory for delta wings with given second derivative of the area distribution at the trailing edge.

Publications of the Aeronautical Research Council

ANNUAL TECHNICAL REPORTS OF THE AERONAUTICAL RESEARCH COUNCIL (BOUND VOLUMES)

- 1941 Aero and Hydrodynamics, Aerofoils, Airscrews, Engines, Flutter, Stability and Control, Structures. 63s. (post 2s. 3d.)
- 1942 Vol. I. Aero and Hydrodynamics, Aerofoils, Airscrews, Engines. 75s. (post 2s. 3d.)
Vol. II. Noise, Parachutes, Stability and Control, Structures, Vibration, Wind Tunnels. 47s. 6d. (post 1s. 9d.)
- 1943 Vol. I. Aerodynamics, Aerofoils, Airscrews. 80s. (post 2s.)
Vol. II. Engines, Flutter, Materials, Parachutes, Performance, Stability and Control, Structures. 90s. (post 2s. 3d.)
- 1944 Vol. I. Aero and Hydrodynamics, Aerofoils, Aircraft, Airscrews, Controls. 84s. (post 2s. 6d.)
Vol. II. Flutter and Vibration, Materials, Miscellaneous, Navigation, Parachutes, Performance, Plates and Panels, Stability, Structures, Test Equipment, Wind Tunnels. 84s. (post 2s. 6d.)
- 1945 Vol. I. Aero and Hydrodynamics, Aerofoils. 130s. (post 3s.)
Vol. II. Aircraft, Airscrews, Controls. 130s. (post 3s.)
Vol. III. Flutter and Vibration, Instruments, Miscellaneous, Parachutes, Plates and Panels, Propulsion. 130s. (post 2s. 9d.)
Vol. IV. Stability, Structures, Wind Tunnels, Wind Tunnel Technique. 130s. (post 2s. 9d.)
- 1946 Vol. I. Accidents, Aerodynamics, Aerofoils and Hydrofoils. 168s. (post 3s. 3d.)
Vol. II. Airscrews, Cabin Cooling, Chemical Hazards, Controls, Flames, Flutter, Helicopters, Instruments and Instrumentation, Interference, Jets, Miscellaneous, Parachutes. 168s. (post 2s. 9d.)
Vol. III. Performance, Propulsion, Seaplanes, Stability, Structures, Wind Tunnels. 168s. (post 3s.)
- 1947 Vol. I. Aerodynamics, Aerofoils, Aircraft. 168s. (post 3s. 3d.)
Vol. II. Airscrews and Rotors, Controls, Flutter, Materials, Miscellaneous, Parachutes, Propulsion, Seaplanes, Stability, Structures, Take-off and Landing. 168s. (post 3s. 3d.)

Special Volumes

- Vol. I. Aero and Hydrodynamics, Aerofoils, Controls, Flutter, Kites, Parachutes, Performance, Propulsion, Stability. 126s. (post 2s. 6d.)
- Vol. II. Aero and Hydrodynamics, Aerofoils, Airscrews, Controls, Flutter, Materials, Miscellaneous, Parachutes, Propulsion, Stability, Structures. 147s. (post 2s. 6d.)
- Vol. III. Aero and Hydrodynamics, Aerofoils, Airscrews, Controls, Flutter, Kites, Miscellaneous, Parachutes, Propulsion, Seaplanes, Stability, Structures, Test Equipment. 189s. (post 3s. 3d.)

Reviews of the Aeronautical Research Council

1939-48 3s. (post 5d.)

1949-54 5s. (post 5d.)

Index to all Reports and Memoranda published in the Annual Technical Reports

1909-1947

R. & M. 2600 6s. (post 2d.)

Indexes to the Reports and Memoranda of the Aeronautical Research Council

Between Nos. 2351-2449

R. & M. No. 2450 2s. (post 2d.)

Between Nos. 2451-2549

R. & M. No. 2550 2s. 6d. (post 2d.)

Between Nos. 2551-2649

R. & M. No. 2650 2s. 6d. (post 2d.)

Between Nos. 2651-2749

R. & M. No. 2750 2s. 6d. (post 2d.)

Between Nos. 2751-2849

R. & M. No. 2850 2s. 6d. (post 2d.)

Between Nos. 2851-2949

R. & M. No. 2950 3s. (post 2d.)

Between Nos. 2951-3049

R. & M. No. 3050 3s. 6d. (post 2d.)

HER MAJESTY'S STATIONERY OFFICE

from the addresses overleaf

© *Crown copyright* 1961

Printed and published by
HER MAJESTY'S STATIONERY OFFICE

To be purchased from
York House, Kingsway, London W.C.2
423 Oxford Street, London W.1
13A Castle Street, Edinburgh 2
109 St. Mary Street, Cardiff
39 King Street, Manchester 2
50 Fairfax Street, Bristol 1
2 Edmund Street, Birmingham 3
80 Chichester Street, Belfast 1
or through any bookseller

Printed in England